in : Progress in physical geography, vol 32, n°4, 2008.p.403-419

Very high-resolution mapping of river-immersed topography by remote sensing

Denis Feurer,[1,2]* Jean-Stéphane Bailly,[1] Christian Puech,[1] Yann Le Coarer[3] and Alain A. Viau[2]

[1]Maison de la Télédétection, 500 rue Jean-François Breton, 34 093 Montpellier Cedex 5, France
[2]GAAP, Pavillon Louis-Jacques Casault, Québec, Québec G1K 7P4, Canada
[3]Cemagref HYAX, 3275 route de Cézanne, CS 40061, 13182 Aix en Provence Cedex 5, France

Abstract: Remote sensing has been used to map river bathymetry for several decades. Non-contact methods are necessary in several cases: inaccessible rivers, large-scale depth mapping, very shallow rivers. The remote sensing techniques used for river bathymetry are reviewed. Frequently, these techniques have been developed for marine environment and have then been transposed to riverine environments. These techniques can be divided into two types: active remote sensing, such as ground penetrating radar and bathymetric lidar; or passive remote sensing, such as through-water photogrammetry and radiometric models. This last technique – which consists of finding a logarithmic relationship between river depth and image values – appears to be the most used. Fewer references exist for the other techniques, but lidar is an emerging technique. For each depth measurement method, we detail the physical principles and then a review of the results obtained in the field. This review shows a lack of data for very shallow rivers, where a very high spatial resolution is needed. Moreover, the cost related to aerial image acquisition is often huge. Hence we propose an application of two techniques, radiometric models and through-water photogrammetry, with very high-resolution passive optical imagery, light platforms, and off-the-shelf cameras. We show that, in the case of the radiometric models, measurement is possible with a spatial filtering of about 1 m and a homogeneous river bottom. In contrast, with through-water photogrammetry, fine ground resolution and bottom textures are necessary.

Key words: immersed topography, remote sensing, river, through-water, very high spatial resolution.

in : Progress in physical geography, vol 32, n°4, 2008.p.403-419

I Introduction

Rivers have a prominent role in many contexts – as a natural environment, as a transfer medium, as a physical medium, as a natural resource. This list is not exhaustive. Understanding the river physical and ecological processes requires knowledge of the three-dimensional geometry of the riverbed, at various spatial and temporal scales, as shown by three examples. First, a key parameter in water resource management is the volume of water flowing in the river and it may be computed by measuring the immersed topography as well as the water level. Second, river morphology monitoring and riverine landscape management requires understanding of underlying physical processes. This is currently done through hydraulic models. These models are most often calibrated or validated with gauging data, which are available at only a few points. The need for detailed knowledge of riverbed topography is hence critically real. Third, when studying processes driving fish population dynamics, the fish habitat approach using spatial data is increasingly used. These spatial models determine, for each fish species and each development stage, the relationship between a presence index and river physical parameters (depth, speed, bottom type) (Le Coarer and Dumont, 1995a). These last two needs are at the root of the work presented hereafter.

Three-dimensional representations of riverbeds are now commonly used in hydrological studies (Lane *et al.*, 1994). Accurate measurement of the river geometry at a large scale, and frequently with very high spatial resolution, is required. If these measures can be obtained from a boat for navigable rivers, the operational fieldwork is tedious. Ground surveys that provide such measurements are time-consuming and necessitate large amounts of manpower. As a consequence, the ratio cost/area covered is very high and investigation is constrained to small parts of the river. As a result, limited funding and working time mean that hydrologic studies cannot be validated for a sufficiently representative section of the river: other solutions to measure river topography have to be investigated.

The scale question shows up quite often in hydrologic studies. Remote sensing has hence been widely used in this domain (Muller *et al.*, 1993; Gendreau and Puech, 2002; Mertes, 2002; Schmugge *et al.*, 2002). Moreover, remote sensing, as a non-contact measurement method, allows one to collect data about an inaccessible river and, in addition, provides complementary data characterizing the river (Creutin, 2001). In the literature river-immersed topography or water depth is often one parameter among others and is rarely the main issue. We have extracted from the literature the information of interest and synthesized it into a review of remote sensing techniques that have been used to map depth and/or riverbed-immersed topography (Table 1).

Excepting sonar, four techniques exist: (1) spectral methods, exploiting the correlation between depth and light absorption; (2) ground penetrating radar (GPR); (3) bathymetric lidar; (4) photogrammetry. These techniques are either active (ie, the illumination is provided by the device) or passive (ie, the illumination is provided by the sun). For each of these techniques, we give a short physical explanation of the method, its applicability, with regard to the different experimental conditions, and finally the measured characteristics, scale, and expectable positioning precision (planimetric and altimetric).

The first part of this paper is a review of the references summarized in Table 1. Thematic applications and remote sensing tools used in these papers are very diverse. In order to deal with such heterogeneous information, the review covers first active remote sensing techniques and then passive ones. In the second part, we present two additional methods, focused on mapping river depth and immersed topography at very high spatial resolution. Indeed, many research issues

in : Progress in physical geography, vol 32, n°4, 2008.p.403-419

Table 1 River bathymetry by remote sensing – case studies

Sites	Platform; sensor	References	Spectral	GPR	Lidar	Stereo
Yukon River, AK, USA	frozen surface; GPR	Annan and Davis (1977)		X		
Willimantic River, CT, USA	boat; 80 MHz GPR	Beres and Haeni (1991)		X		
St Mary River, MI, USA	plane; Daedalus 1260	Lyon *et al*. (1992)	X			
Green River, UT, USA	plane; COHU 4810	Hardy *et al*. (1994)	X			
Faith Creek, AK, USA	plane; Hamamatsu	Gilvear *et al*. (1995)	X			
Rupnarayan-Hooghly river confluence, India	satellite; IRS-1b LISS-II	Kumar *et al*. (1997)	X			
Southwestern WA, USA	cable; 100 MHz GPR	Spicer *et al*. (1997)		X		
River Tummel, Scotland	plane; ATM, B&W photo	Winterbottom and Gilvear (1997); Gilvear *et al*. (2004)	X			
Saco River, Maine	helicopter; SHOALS	Irish and Lillycrop (1999)			X	
River Tay, Scotland	plane; ATM, B&W photo	Bryant and Gilvear (1999)	X			
Harrison and Horsefly Rivers, BC, Canada	plane; 3 CCD cameras + imaging spectrometer VIFIS	Roberts and Anderson (1999)	X			
Skagit River, WA, USA	cable; 100 MHz GPR	Costa *et al*. (2000); Haeni *et al*. (2000)		X		
Ashburton River, New Zealand	plane; Zeiss LMK15	Westaway *et al*. (2000; 2001)				X
Cowlitz River, WA, USA	helicopter; 100 MHz GPR	Melcher *et al*. (2002)				
Lamar River, WY, USA	helicopter; Probe-1	Marcus *et al*. (2003)	X			
Waimakariri River, New Zealand	plane; Zeiss LMK15	Westaway *et al*. (2003)	X			
Durance, France	UAV; non-metric 35 mm camera	Chaponnière (2004)	X			
River Tummel, Scotland	plane; 35 mm colour camera and daedalus 1260	Gilvear *et al*. (2004)	X			
Soda Butte Creek , WY, USA	helicopter; ADAR and Probe-1	Legleiter *et al*. (2004)	X			
Sagavanirktok River, AK, USA	frozen surface; GPR	Lunt and Bridge (2004)		X		

(*Continued*)

Table I (*Continued*)

Sites	Platform; sensor	References	Spectral	GPR	Lidar	Stereo
Colorado River, CO, USA	helicopter; SHOALS 1000-T	Davis *et al.* (2005)			X	
Tofino Creek, BC, Canada	plane; CASI	Leckie *et al.* (2005)	X			
Yakima River, WA, USA	plane, helicopter; SHOALS 1000-T	Millar *et al.* (2005)			X	
Lamar River, WY, USA	plane; AISA	Legleiter and Roberts (2005)	X			
Sainte-Marguerite River, QC, Canada	helicopter; XEOS	Carbonneau *et al.* (2006)	X			
Middle Fork Salmon River, ID, USA	plane; EAARL	McKean *et al.* (2006)			X	
Platte River, NE, USA	plane; EAARL	Kinzel *et al.* (2007)			X	
Ain and Drôme Rivers, France	UAV; Canon Powershot G5	Lejot *et al.* (2007)	X			

remain: in short, active methods imply heavy logistics and great costs, and hence have been first studied with simulated data rather than in the field (Lesaignoux, 2006; Lesaignoux *et al.*, 2007). Meanwhile, for local-scale hydrologic studies, in small streams, where centimetric precision is required, there is a big issue in assessing the potential of very high spatial resolution imagery as a tool to map river depth or immersed topography. This is the topic of the two studies presented in the second part of this paper.

II Review of the remote sensing techniques for bathymetry

Most methods employed in the riverine environment have first been developed and tested for the marine environment (Hickman and Hogg, 1969; Polcyn *et al.*, 1970; Lyzenga, 1978; Fryer, 1983; Morel, 1998). The theoretical background of the methods described hereafter comes largely from these works. The review is divided into two parts: first, the theoretical background of each method; second, the experimental results obtained in terms of feasibility, characteristics and quality of the measure.

1 Principle of the different methods

a Spectral methods: These methods, using passive optical imagery, are based on the fact that light is attenuated through the water column. Thus, image information is related to water depth. As a consequence, these methods do not give access to the absolute position of the river bottom (river-bed topography). Several publications have proposed methods based on image classification (Hardy *et al.*, 1994; Marcus *et al.*, 2003; Gilvear *et al.*, 2004; Leckie *et al.*, 2005). In these works, depth is a descriptive parameter among others, such as bottom type or hydrodynamic unit. The main objective is often to map and characterize the river and its habitats.

A second method, with a physical background, has also been quite widely used.

When the effects due to scattering in the water and internal reflection at the water surface ere neglected, light energy decreases exponentially through the water column (Polcyn *et al.*, 1970; Lyzenga, 1978). Lyzenga (1978) thus proposed using a variable, defined by Xi = ln (Li – Lio), with i, spectral band index; Li, radiance measured by the sensor; Lio, radiance of a theoretical infinite water column. The Xi variable is approximately linearly correlated to the depth. Remaining internal reflection effects are significant only for very shallow water and high bottom reflectance. For a given wavelength, atmospheric condition and bottom type, extinction depth value depends on the attenuation coefficient of the water, which mainly depends on water turbidity. Hence, the possibility of measuring depth strongly depends on turbidity conditions.

In addition, an interesting piece of work should be cited here, even though it has not yet been applied to riverine environments. Morel (1998) proposed a method to derive water depth from remote sensing images without in situ measured depths. The method, called 4SM, uses shallow areas of the image to derive ratios Xi/Xj for all pairs of spectral wavelengths i and j. With these data and the attenuation coefficients given by Jerlov (1976), a digital elevation model and a low-tide view (corresponding to bottom reflectance) are computed.

b Stereophotogrammetry: Photogrammetry includes a set of techniques for deriving spatial information from images. Among these techniques, stereorestitution consists of determining terrain elevation from several pictures of the same area taken with different viewing angles. Indeed, within two images of the same area, one – motionless – point will have a different location because of: (1) the sensors' internal characteristic differences (if two different sensors are used); (2) different positions of the two sensors; (3) different viewing angles; (4) point relative height (see Figure 1).

It is thus possible to calculate point heights from their positions within the two images. The information needed is: (1) positions of the image points; (2) sensor internal geometry; (3) sensor external geometry.

In the particular case of through-water photogrammetry, the air/water interface implies additional processing. Refraction

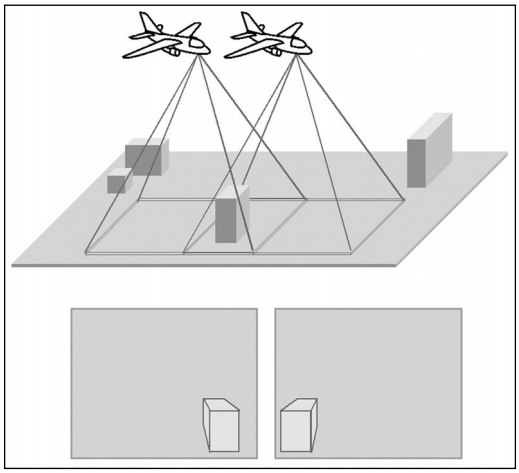

Figure 1 The stereoscopic effect: image acquisition (3D); stereo pair (2 × 2D)

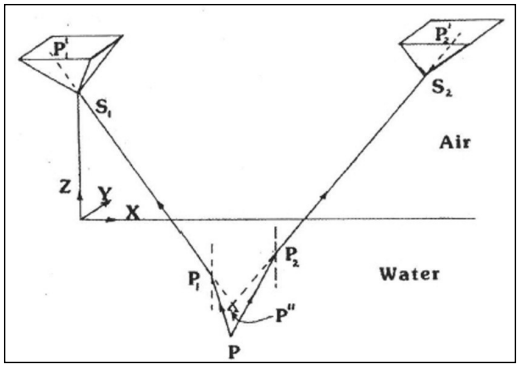

Figure 2 Geometry of through-water photogrammetry (from Fryer, 1983). P is the actual position of the immersed point, P'' is the apparent point. P_1 and P_2 are the intersections of light rays with the water surface. S_1 and S_2 are the optical centres of the two cameras. P'_1 and P'_2 are the image points of the point P

through water surface leads to apparent depths inferior to the actual ones (see Figure 2, where P˝ is the apparent position of P). Waves and specular reflection add extra error sources (Okamoto, 1982; Fryer, 1984; 1985; Feurer *et al*., 2007).

c Ground penetrating radar (GPR): The principle of ground penetrating radar is the following (see Figure 3): one antenna generates an electromagnetic wave, which is transmitted, absorbed and reflected by the media and interfaces between two media. The part of the energy returning to the sensor is received by the antenna and recorded. Record shape (echo amplitude and/or two-way time – see Figure 4) allows one to determine the geometry of the crossed media. For instance, interfaces between two media provoke strong reflections that are generally easily detectable. A quite detailed understanding of the physics associated can be found in Davis and Annan (1989).

GPR was first developed for geological studies, and its use was then extended to hydrogeological and hydrological studies. It has also been used to measure lake or river depths, either when their surface is frozen or during flood events. Physically, both the air/water and the water/ground interfaces return echoes, so water thickness can be measured.

d Lidar (Light detection and ranging): Lidar is the name of an active sensor. Two pulses of different wavelengths are sent out. The near-infrared one only penetrates a few centimetres and is hence quickly attenuated and returned by the water surface. The green one penetrates the water and is returned by the bottom. Measuring the signal travel times allows calculation of the water depth (see Figure 5).

Laser pulses are deflected by a rotating mirror, which allows ground scanning across the flight line, in front of the platform. Water depth calculation algorithms can use various

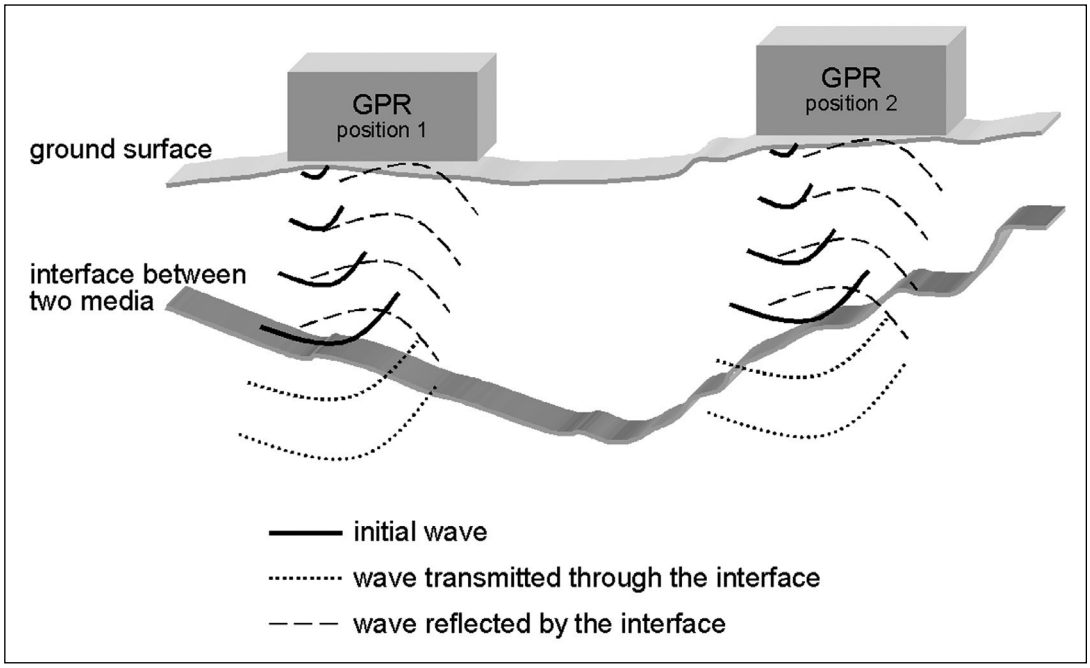

Figure 3 The principle of ground penetrating radar (GPR)

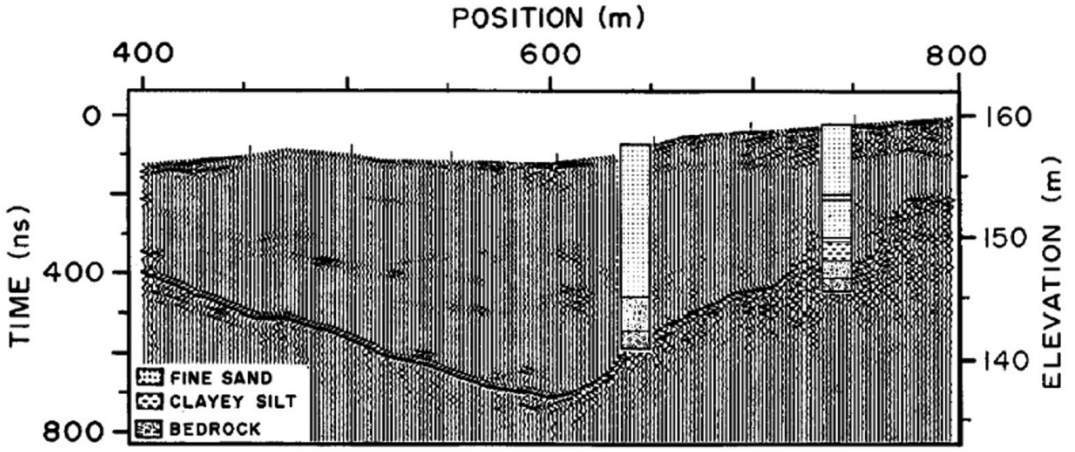

Figure 4 Example of record obtained by GPR (Davis and Annan, 1989). Every single return full waveform has been put vertically side by side so that the whole cross-section is described

wave returns (Pe'eri and Philpot, 2007; Allouis and Bailly, 2008): (1) infrared return: strongly absorbed, penetrates very little in water, used to determine the air/water interface; (2) red return: due to Raman diffusion, characterizes the volume diffusion; (3) first green return: water interface slightly reflects the green pulse – when significant, this first green return can help in the localization of the water surface; (4) last green return, corresponding to river bottom.

The bibliography for bathymetric lidar is essentially focused on applications in coastal marine environment (for instance, Hoge *et al.*, 1980; Lyzenga, 1985; Muirhead and Cracknell, 1986; Irish and Lillycrop, 1997; 1999; Parson *et al.*, 1997; Irish and White, 1998; Cracknell, 1999, Guenther *et al.*, 2000; Buonaiuto and Kraus, 2003; Fitzgerald *et al.*, 2003; Storlazzi *et al.*, 2003). As noticed by Wozencraft and Millar (2005), lidar river bathymetry remains rare. At present the only two peer-reviewed works are Hilldale and Raff (2007) and Kinzel *et al.* (2007). In addition, one can find an increasing number of conference/workshop presentations (Millar *et al.*, 2005; McKean *et al.*, 2006; Pe'eri and Philpot, 2007; Bailly *et al.*, 2008).

2 Measurement characteristics and scale – applicability

a Potential of passive optical imagery: spectral methods and stereophotogrammetry: Applicability of these methods mainly depends on the solar energy transmitted through the water column and reflected by the river bottom, which must be visible. As a consequence, measurement is severely limited in turbid waters, locally impeded by overhanging vegetation or specular reflections (sun glints); maximum measurable depth depends on water clarity. As noticed by Lejot *et al.* (2007), a limit of around 1 m is often reported for gravel-bed rivers (Winterbottom and Gilvear, 1997; Brasington *et al.*, 2003), but some experiments have been done for rivers deeper than 3 m (Lyon *et al.*, 1992; Lejot *et al.*, 2007), and even 10 m (Kumar *et al.*, 1997). These techniques perform a pixel-based image analysis. Thus, depth measurement is spatialized on a regular grid. Depth measurement planimetric resolution ranges from 5.6 cm (Brasington *et al.*, 2003) to 36.25 m (Kumar *et al.*, 1997), depending on sensor and data processing. Using images implies finding a compromise

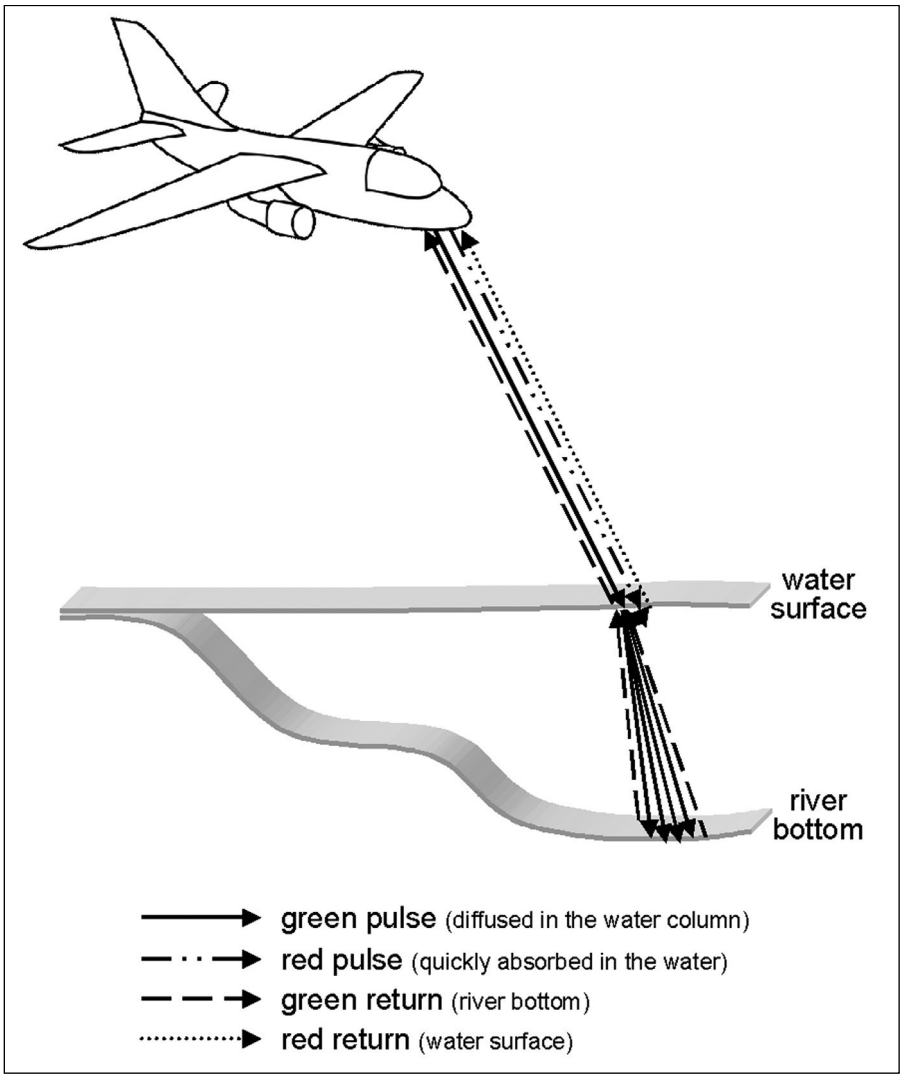

Figure 5 The principle of lidar

between planimetric resolution and spatial coverage of each image (and thus global cost). As reported by Gilvear *et al.* (2004), data processing strongly depends on study site and experiment conditions (bottom spectral heterogeneity, turbidity), and error sources are diverse (riparian vegetation shadows, sun glints). Most often, the results are qualified by giving the correlation between observed and computed data. A few references qualify the results in terms of mean error and standard deviation of the errors. With very high spatial resolution (centimetric ground pixels), measure precision is no better than 20 cm and measure accuracy around 10 cm. Working scales mainly depend on sensors and platforms used. For large streams (over 200 m wide), satellite imagery can be used. For smaller streams (between 20 and 200 m wide), airborne remote sensing is used.

Works dealing with remote sensing of smaller streams are less numerous, because of spatial resolution limitations (Gilvear *et al*., 2004).

b Potential of GPR: Following the work of Annan and Davis (1977), Kovacs (1978) measured water depths up to 5 m under 2 m thick ice, and Moorman and Michel (1997) measured water depths up to 20 m, both on frozen lakes. Most often, GPR is used very close to the surface of the river, frozen river, bridge, cable, or low-flying helicopter. At present, only one reference to GPR mounted on a helicopter exists (Melcher *et al*., 2002). GPR is most often used along a transect (cable, bridge). Creutin (2001) mentioned a survey in which a 200 m long transect was measured within 10 minutes. Using a helicopter, Melcher *et al*. (2002) flew over three sites spanning 100 km within 60 minutes (characteristics of each site are not given). Resolution in elevation mainly depends on the frequency used. The higher the frequency, the higher is the resolution, approximately a third of the wavelength: with a 100 MHz radar, vertical resolution is about 10 cm (Spicer *et al*., 1997). Due to the fact that water depth is derived from a travel time, precision and accuracy of the measure depend on how well the medium characteristics are known. Penetration depth is best for low water conductivities and low electromagnetic wave frequencies. This leads (see above) to a compromise between penetration depth and vertical resolution. Penetration depth in pure water with a 100 MHz GPR is about 10 m (Spicer *et al*., 1997). GPR can be used through only low-conductivity water, less than 1000 S cm^{-1}, and sediment concentration lower than 10,000 mg L^{-1} (Creutin, 2001).

c Potential of bathymetric lidar: This method encounters the same limitations as passive optical ones concerning the overhanging vegetation, but does not depend on illumination conditions (Hilldale and Raff, 2007). Nevertheless, this technique is still sensitive to water turbidity. Energy of laser pulse allows the penetration of the water column only typically up to two or three times the Secchi depth. The technique involves algorithms that detect and discriminate energy peaks, which is hardly possible for depths lower than 0.50 m (Lesaignoux *et al*., 2007). Depth measures obtained with bathymetric lidar consist of a non-regular point cloud. Laser pulse footprints have a typical 2 m diameter extent. It is larger on the river bottom because of light dispersion and refraction through water. The planimetric positioning accuracy of each spot ranges from 1 to 5 m depending on the positioning technology used (see Irish and Lillycrop, 1999, for SHOALS specifications). Vertical accuracy is minimally 0.20 m. Swath width depends on the sensor, acquisition mode and flight height. It is roughly included within the range of 0.5 to 0.75 h where h is the flight height. Ordinarily, flight height is about 200 to 500 m, which gives about 100 to 400 m swath widths. The area covered within one hour ranges from about 20 to 60 km^2.

3 Synthesis

This review shows that, among the four methods presented, the majority of studies concern the spectral methods. Some very specific applications use GPR. In addition, river applications of bathymetric lidar are becoming more numerous. There is a crucial lack of experiments in through-water photogrammetry, with only one test, on the Ashburton River, New Zealand (see Table 2).

In addition, it is noticeable that image acquisition from ultra-light aircrafts or unmanned aerial vehicles (UAV), with off-the-shelf sensors, is still very new in the literature (Lejot *et al*., 2007). Hence, we decided to test the two passive methods with this specific equipment, easily exploitable in field and affordable for the majority.

Table 2 River depth mapping by remote sensing: characteristics of each method

Technique	Measure density	Accuracy	Data acquisition	Applicability	Remarks
Lidar	2×2 m to 5×5 m	XY: 1 to 2.5 m Z: 0.18 to 0.35 m	1 hour for 70 km^2	0.5 to 60 m according to turbidity, no overhanging vegetation	in development for shallow waters
GPR	depends on protocol	Z: 0.30 m at 100 MHz (estimated)	2 $m.s^{-1}$ along a cable, airborne in test	turbid and flooding rivers	vertical precision decreases with max. penetration depth
Spectral	pixel size (5.6 cm to 36.25 m)	XY: subpixel Z: highly variable (min. 0.20 m)	aerial or satellite imagery	clear water, homogeneous bottoms, no overhanging vegetation	need for calibration data
Photogrammetry	pixel size	XY: subpixel Z: 0.20 cm	aerial imagery, 60% overlap	clear water, homogeneous bottoms, no overhanging vegetation	data taken from the unique available reference

III Case study of small-scale river bathymetry with small-format cameras and ultra-light aircraft

1 Test site and data acquisition

The test site is located on the middle Durance River, France. This part of the river is a 60 km long regulated stretch, downstream of the Serre-Ponçon dam. Water level and discharge are fairly low and constant in the natural bed of the river and the shallow waters are usually clear. Four tributaries still bring small natural variations, so this section was chosen as a test site for hydrobiological studies. River width varies between 5 and 100 m. The mean depth is around 0.30 m, with maximum depths around 2 m. Our study was focused on two test sites of about 1 km length (see Figure 6). On these two test sites, depth varies from 0 to 1.6 m with a mean of 0.26 m; width ranges from 10 to 50 m.

Images were acquired from ultra-light aircrafts and UAVs. Such aircraft can fly relatively slowly and low. In addition, such aerial platforms allow acquisition at a reduced cost and improve the acquisition flexibility. Usually, UAVs are considered as scale models and benefit from lighter regulation. Images treated with the radiometric method were acquired for September 2004, with a 35 mm film NIKON F100 camera aboard a Pixy (Asseline *et al*., 1999). We used natural colour, colour infrared, and tungsten films, which cover various spectral bands. Flying heights were between 50 and 150 m, giving ground resolutions between 1 and 3 cm. Some targets (black and white test cards) were installed in the field in order to retrieve acquisition geometry.

A second image acquisition campaign was held in September 2005, with a view to testing the photogrammetric method. We used a Sony DSC-F828 small-format non-metric digital camera. We also used a polarizing filter in order to limit sun glints. The sensor was fixed on a custom-built platform, hand-held off board a Ballerit HM-1000 ultra-light aircraft. Within such conditions

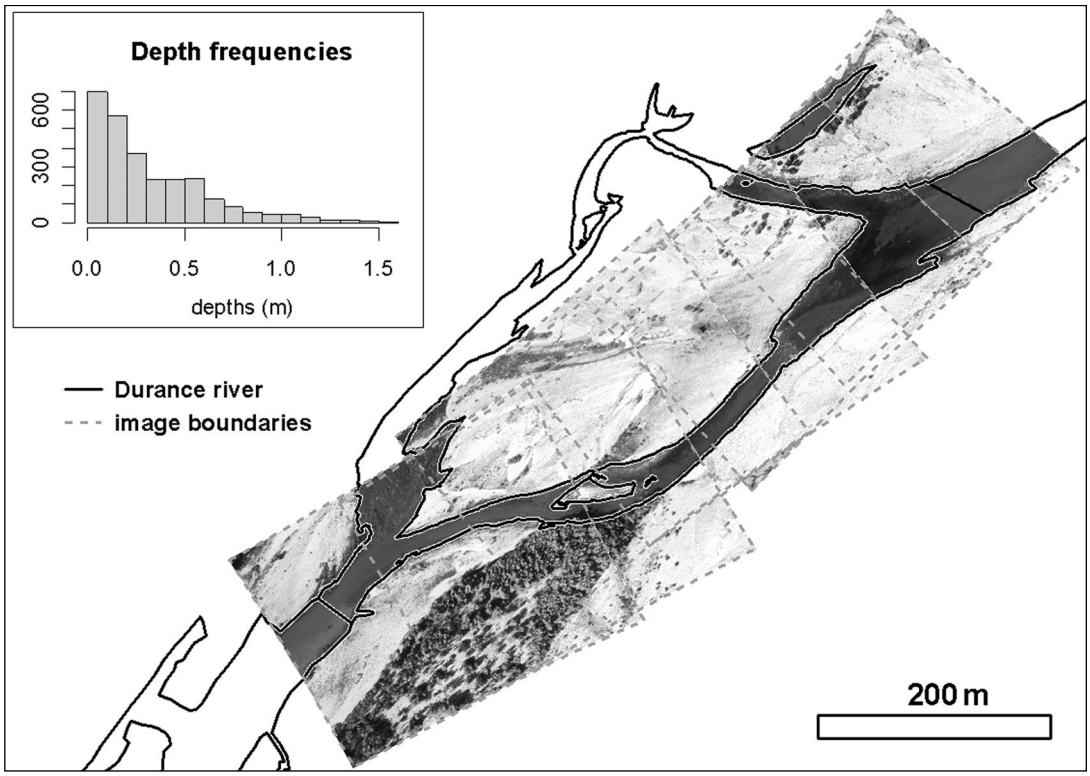

Figure 6 Test site on the Durance River and left channel depth distribution (histogram). The river flows from top right to bottom left. An image band is superimposed on the left channel

Source: Images from http://www.lavionjaune.fr

the photographer is able to set the rotation of the polarizing filter and even rectify the position of the platform to the near vertical in real time. About 200 red crosses were painted as ground control points. Flying height and speed were fixed, and a timing interval was determined in order to obtain consistent flying axes with 60% overlapping. With an average flying height of 220 m, the ground resolution is approximately 0.09 cm. Independent validation data sets were acquired with a Leica TCRA1102 total station, according to the method published by Le Coarer and Dumont (1995b). Ground control points have been positioned with either the same equipment or a Leica 1200 differential GPS in RTK mode.

2 Methodology

a Radiometric models: Using Lyzenga's (1978) method, Winterbottom and Gilvear (1997) exploited the logarithmic relationship between image reflectance and water depth through regression analysis. Orthophotos were produced with ERDAS Imagine Orthobase, thanks to the ground control points visible in the images. Three image blocks, corresponding to the three film types colour infrared, tungsten, and natural colours), were formed. These stereo models have RMSE of 2.26 (colour infrared), 2.88 (tungsten) and 3.87 pixels (natural colours), with ground pixel sizes respectively of 1 cm, 2 cm and 1 cm. Once the georeferencing step

was done, the regression analysis between image data and ground truth followed. One-third of the ground truth points were saved as an independent validation data set. The remaining two-thirds were used to determine the relationship between radiometry and water depth. Two sub-areas (pools and riffles) for each image were analysed. The coefficients A, B, C and D of the following equation were determined for each image and each sub-area:

$$\text{Depth} = A * \ln(R) + B * \ln(G) + C * \ln(B) + D$$

with R, G and B the red, green and blue image bands.

The first regressions performed on a pixel base showed R^2 values ranging from 0.2 to 0.5 depending on photographic emulsion and river sector. When comparing the depths predicted by these models to the actual ones, the correlation ranges between 0.23 and 0.60. Analysis of differences between predicted and actual depths shows a strong sensitivity of the regression laws to features such as residual sun glints or local algal cover. To reduce the effect of these local features, different median spatial filters, with window sizes from 1×1 to 200×200 pixels, were used. The same regression analysis was done for each of these window sizes.

b Through-water photogrammetry: This method takes advantage of the image geometric information. Knowing the acquisition geometry and the position of a point within two images, the (x, y, z) position of this point can be computed. In the case of a riverbed, an additional issue has to be taken into account: refraction of light rays through the air/water interface. In order to measure depths from the set of images, we followed a three-step procedure: (1) geometric calibration; (2) stereo measurement; (3) processing of the refraction effect. Interior calibration consisted of lens distortion correction, and determination of the position of the CCD matrix relatively to the body of the camera and the optical system. Exterior orientation was done for each stereo pair with bundle adjustment. Stereorestitution implies image point identification between the two images. This can be accomplished with automatic matching algorithms or by manual stereo matching. For the latter technique, we used special glasses and software allowing the operator to see the stereo model in relief. The main advantage of the latter technique is the noticeable reduction of false matching. Finally, the effect of refraction was taken into account. Interface position was derived from the bank lines. Given the positions of the river bed point, of the interface, and the stereo pair acquisition parameters, it was possible to compute the geometry of incident rays and thus the intersection of refracted rays (Feurer *et al*., 2008).

3 Potential of the methods

a Radiometric models: An optimal window size between 50 and 100 pixels occurred for both the riffles and pools (Figure 7). This corresponds to an approximate ground resolution between 1 and 2 m. This is consistent with the results obtained by Carbonneau *et al*. (2006) on the same type of river. The regression laws corresponding to the optimal coefficient of determination were then used to produce depth maps. More than 500 independent immersed points were used for the validation, within the different sectors of the river, and for the different film emulsions. The mean error ranged between 0.03 and 0.13 m. The root mean square error ranged between 0.04 and 0.16 m. The detailed error statistics are summarized in Table 3. As a comparison, actual depths ranged between 0 and 0.90 m, with a standard deviation of 0.22 m and a mean value of 0.40 m. There are still residual errors related to sun glint and algal cover, which are not taken into account by the logarithmic model. A way

Table 3 Radiometric method: comparison with an independent ground truth data set; RMSE is for root mean square error and ME for mean error

Emulsion	Riffles	Pools
colour infrared pixel: 1 cm	RMSE: 0.04 cm ME: 0.03 cm	RMSE: 0.16 cm ME: 0.13 cm
natural colours pixel: 1 cm	RMSE: 0.07 cm ME: 0.05 cm	RMSE: 0.09 cm ME: 0.07 cm
tungsten pixel: 2 cm	RMSE: 0.06 cm ME: 0.04 cm	RMSE: 0.13 cm ME: 0.10 cm

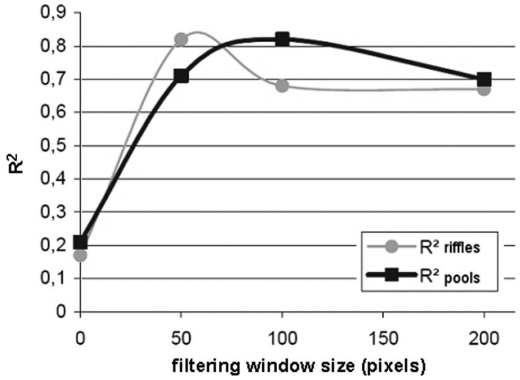

Figure 7 Determination of the optimal spatial resolution for the radiometric models method

to improve these results is to refine the algorithm by applying different regressions to more numerous sectors, for instance sectors showing bright and dark bottoms. This has been tested on one natural-colour image and decreased the RMSE from to 0.09 to 0.06 m in the pools with bright bottoms.

b Through-water photogrammetry: Interior orientation and lens calibration was done from four stereo pairs of a known scene, including 50 points in three points, whose position is known with a millimetric accuracy. The Etalonnage software (Egels, 2000) allowed reduction of the RMSE of the models from 5 to 0.25 pixels by taking into account a radial distortion. The exterior orientation parameters were determined for each of the nine stereo pairs covering the full 800 m long reach by the Poivilliers E software, described in Egels (2000). The residual parallax of each stereo model ranged from 0.17 to 0.85 pixels. Due to turbidity and clogging conditions, the distribution of matched points was not uniform. Due to diffusion phenomenon linked to water turbidity, the 0.09 m ground resolution hardly allowed the detection of individual cobble or pebble. Typically, these objects could have been pointed out in very shallow waters, where their sharp shadow provided a good contrast. In deeper waters, the matched points corresponded most often to a limit between algal cover and bottom without immersed vegetation.

The mean error on the whole reach was 0.10 m. The standard deviation of the error was 0.19 m. The deviation of the error was 0.13 m for stereo pairs with better acquisition condition (B/h ratios around one), which should be compared to 0.20 m, the standard deviation of the error for the stereo pairs with a B/h around 0.50. A positive bias can be noticed for all the stereo pairs. This systematic error can be explained by several factors. The river bottom surveyed in field is filtered; indeed, operators survey the mean bottom level and avoid taking into account the local variations due to an isolated rock or immersed vegetation covering the riverbed. In addition, in the case of this experiment, most points were taken on the edge of a vegetated area, which increased the relative influence of these areas. This requires further study, in particular with different acquisition geometries and scales allowing the detection of individual rocks and coarse pebbles.

IV Conclusion

This review shows that, among the four presented methods, most studies concern spectral methods; most often, data acquisition is from a plane. In the light of this work, we decided to test the two passive methods with very high spatial resolution and specific equipment easily exploitable in field and affordable for the majority. The first study, described with more detail in Chaponnière (2004), used radiometric models extrapolated at the image scale from calibration points. This work showed that the smallest ground resolution is not the most effective; ground pixels of about 1 m seem indeed to produce the best results. This leads to the conclusion that very high-resolution satellite imagery is a fair compromise when using such models.

The second study, whose method was presented in Feurer *et al*. (2008), showed that through-water photogrammetry is possible with such platforms and cameras, with special care taken about geometric calibration and refraction correction. On the other hand, measure precision is proportional to the ground resolution, and measure accuracy is critically sensitive to the geometry acquisition and the accuracy of these parameters when computed from ground control points. Some improvements must therefore be done on the control of these parameters in order to obtain a satisfactory accuracy and precision for long flight lines.

Finally, the bathymetric lidar, which was not tested here, appears as a very interesting tool to monitor river bathymetry, because active laser allows measurement even within bad illumination conditions or with low turbidity. On the other hand, its ability to map depth lower than 0.50 m has not yet been demonstrated. For smaller depths, the use of other algorithms and other wavelengths (such as a red one, to detect the Raman diffusion peak, for instance) is necessary (Pe'eri and Philpot, 2007; Allouis *et al*., 2008).

References

Allouis, T. and **Bailly, J.** 2008: On the use of Raman, infra-red, and green waveforms in bathymetric LiDAR for very shallow waters. In European Geosciences Union (EGU) General Assembly, 14–18 April, Vienna.

Annan, A. and **Davis, J.** 1977: Impulse radar applied to ice thickness measurements and fresh water bathymetry. Technical report, Current Research Part B, GSC Paper 77-1b, Geological Survey of Canada, 63–65.

Asseline, J., de Noni, G. and **Chaume, R.** 1999: Conception et utilization d'un drone à vol lent pour la télédétection rapprochée. *Photo Interprétation* 37, 3–13.

Bailly, J., Le Coarer, Y., Allouis, T., Stigermark, C.J., Languille, P. and **Adermus, J.** 2008: Bathymetry with LiDAR on gravel bed-rivers: quality and limits. In European Geosciences Union (EGU) General Assembly, 14–18 April, Vienna.

Beres, M.J. and **Haeni, F.** 1991: Application of ground-penetrating-radar methods in hydrogeologic studies. *Ground Water* 29, 375–86.

Brasington, J., Langham, J. and **Rumsby, B.** 2003: Methodological sensitivity of morphometric estimates of coarse fluvial sediment transport. *Geomorphology* 53, 299–316.

Bryant, R.G. and **Gilvear, D.J.** 1999: Quantifying geomorphic and riparian land cover changes either side of a large flood event using airborne remote sensing: River Tay, Scotland. *Geomorphology* 29(38445), 307–21.

Buonaiuto, F. and **Kraus, N.** 2003: Limiting slopes and depths at ebb-tidal shoals. *Coastal Engineering* 48, 51–65.

Carbonneau, P.E., Bergeron, N. and **Lane, S.N.** 2006: Feature based image processing methods applied to bathymetric measurements from airborne remote sensing in fluvial environments. *Earth Surface Processes and Lamdforms* 31, 1413–23.

Chaponnière, P. 2004: Télédétection et bathymétrie des rivières: application à la Durance. Master's thesis, Ecole Nationale Supérieure de Géologie (ENSG).

Costa, J.E., Spicer, K.R., Cheng, R.T., Haeni, P.F., Melcher, N.B., Thurman, M.E., Plant, W.J. and **Keller, W.C.** 2000: Measuring stream discharge by non-contact methods: a proof-of-concept experiment. *Geophysical Research Letters* 27, 553–56.

Cracknell, A. 1999: Remote sensing techniques in estuaries and coastal zones-an update. *International Journal of Remote Sensing* 20, 485–96.

Creutin, J. 2001: Local remote sensing of rivers (418). Technical Report, IIHR-Hydroscience and Engineering, University of Iowa.

Davis, J.L. and **Annan, A.** 1989: Ground-penetrating radar for high-resolution mapping of soil and rock stratigraphy. *Geophysical Prospecting* 37, 531–51.

Davis, P.A., Gonzales, F.M., Brown, K.M. and **Melis, T.S.** 2005: Evaluation of the SHOALS 1000T bathymetric LIDAR system for monitoring channel sediment within the Colorado River in Arizona. In American Geophysical Union (AGU) Fall meeting.

Egels, Y. 2000: Photogrammétrie et micro-ordinateur. *XYZ* 82, 31–35.

Feurer, D., Bailly, J., Le Coarer, Y., Puech, C. and **Viau, A.A.** 2007: On the use of very high resolution optical images to map river bathymetry: upscaling from aerial to satellite imagery. In Second Space For Hydrology Workshop 'Surface water storage and runoff: modeling, in-situ data and remote sensing', 12–14 November, Geneva.

Feurer, D., Bailly, J. and **Puech, C.** 2008: Measuring depth of a clear, shallow, gravel-bed river by through-water photogrammetry with small format cameras and ultra light aircrafts. In *Geophysical Research Abstracts* 10, European Geosciences Union (EGU) General Assembly, 14–18 April, Vienna.

Fitzgerald, D., Zarillo, G. and **Johnston, S.** 2003: Recent developments in the geomorphic investigation of engineered tidal inlets. *Coastal Engineering Journal* 45, 565–600.

Fryer, J. 1983: Photogrammetry through shallow water. *Australian Journal of Geodesy, Photogrammetry and Surveying* 38, 25–38.

— 1984: Errors in depth determined by through-water photogrammetry. *Australian Journal of Geodesy, Photogrammetry and Surveying* 40, 29–39.

— 1985: Errors in depth determination caused by waves in through-water photogrammetry. *Photogrammetric Record* 11, 745–53.

Gendreau, N. and **Puech, C.** 2002: Hydrology and remote sensing information. *Houille Blanche-Revue Internationale de l'Eau* 1, 31–34.

Gilvear, D.J., Davids, C. and **Tyler, A.N.** 2004: The use of remotely sensed data to detect channel hydromorphology. River Tummel, Scotland. *River Research and Applications* 20, 795–811.

Gilvear, D.J., Waters, T.M. and **Milner, A.M.** 1995: Image analysis of aerial photography to quantify changes in channel morphology and instream habitat following placer mining in interior Alaska, Freshwater Biology 34, 389–98.

Guenther, G., Brooks, M. and **LaRocque, P.E.** 2000: New capabilities of the 'SHOALS' airborne lidar bathymeter. *Remote Sensing of Environment* 73, 247–55.

Haeni, F., Buursink, M.L., Costa, J.L., Melcher, N.B., Cheng, R.T. and **Plant, W.J.** 2000: Ground-penetrating radar methods used in surface-water discharge measurements. In Noon, D.A., Stickley, G.F. and Longstaff, D., editors, *GPR 2000*, 8th International Conference on Ground Penetrating Radar, Gold Coast, Australia, 494–500.

Hardy, T.B., Anderson, P.C., Neale, M.U. and **Stevens, D.K.** 1994: Application of multispectral videography for the delineation of riverine depths and mesoscale hydraulic features. In Marston, R. and Hasfurther, V., editors, *Effects of human-induced changes on hydrologic systems*, Symposium of the American Water Resources Association, Jackson Hole, Wyoming, 445–54.

Hickman, G.D. and **Hogg, J.E.** 1969: Application of an airborne pulsed laser for near shore bathymetric measurements. *Remote Sensing of Environment* 1, 47–58.

Hilldale, R.C. and **Raff, D.** 2007: Assessing the ability of airborne LiDAR to map river bathymetry. *Earth Surface Processes and Landforms* 33, 773–83.

Hoge, F., Swift, R.N. and **Frederick, E.B.** 1980: Water depth measurement using an airborne pulsed neon laser system. *Applied Optics* 19, 871–83.

Irish, J. and **Lillycrop, W.** 1997: Monitoring New Pass, Florida, with high density lidar bathymetry. *Journal of Coastal Research* 13, 1130–40.

— 1999: Scanning laser mapping of the coastal zone: the SHOALS system. *ISPRS Journal of Photogrammetry and Remote Sensing* 54, 123–29.

Irish, J. and **White, T.** 1998: Coastal engineering applications of high-resolution lidar bathymetry. *Coastal Engineering* 35, 47–71.

Jerlov, N. 1976: *Marine optics*. Amsterdam: Elsevier.

Kinzel, P.J., Wright, C.W., Nelson, J.M. and **Burman, A.R.** 2007: Evaluation of an experimental LiDAR for surveying a shallow, braided, sand-bedded river. *Journal of Hydraulic Engineering* 133, 838–42.

Kovacs, A. 1978: Remote detection of water under ice-covered lakes on the north slope of Alaska. *Arctic* 31, 448–58.

Krauss, K. and **Waldhäusl, P.** 1998: *Manuel de photogrammétrie*. Paris: Editions Hermès.

Kumar, V.K., Palit, A. and **Bhan, S.** 1997: Bathymetric mapping in Rupnarayan-Hooghly river confluence using Indian remote sensing satellite data. *International Journal of Remote Sensing* 18, 2269–70.

Lane, S., Chandler, J. and **Richards, K.** 1994: Developments in monitoring and modelling small-scale river bed topography. *Earth Surface Processes and Landforms* 19, 349–68.

Leckie, D., Cloney, E., Jay, C. and **Paradine, D.** 2005: Automated mapping of stream features with high-resolution multispectral imagery: an example of the capabilities. *Photogrammetric Engineering and Remote Sensing* 71, 145–55.

Le Coarer, Y. and **Dumont, B.** 1995a: Virtual rivers for the study of aquatic fauna. *Ingénieries* 2, 21–28.

— 1995b: Modelling stream morphodynamics for research in habitat-aquatic fauna relationships.

Bulletin Français de la Pêche et de la Pisciculture 337/339, 309–16.

Legleiter, C. and **Roberts, D.** 2005: Effects of channel morphology and sensor spatial resolution on image-derived depth estimates. *Remote Sensing of Environment* 95, 231–47.

Legleiter, C., Roberts, D.A., Marcus, A.W. and **Fonstad, M.A.** 2004: Passive optical remote sensing of river channel morphology and in-stream habitat: physical basis and feasibility. *Remote Sensing of Environment* 93, 493–510.

Lejot, J., Delacourt, C., Piégay, H., Fournier, T., Trémélo, M. and **Allemand, P.** 2007: Very high spatial resolution imagery for channel bathymetry and topography from an unmanned mapping controlled platform. *Earth Surface Processes and Landforms* 32, 1705–25.

Lesaignoux, A. 2006: Modélization et simulations de trains d'ondes LiDAR 'vert': application à la détection de faibles lames d'eau en rivière. Master's thesis, Université Montpellier II – CNAM.

Lesaignoux, A., Bailly, J. and **Feurer, D.** 2007: Small water depth detection from green lidar simulated full waveforms: application to gravel-bed river bathymetry. In Physics in Signal and Image Processing (PSIP) Fifth Internation Conference, 31 January–2 February, Mulhouse, France.

Lunt, A. and **Bridge, J.** 2004: Evolution and deposits of a gravelly braid bar, Sagavanirktok River, Alaska. *Sedimentology* 51, 415–32.

Lyon, J.G., Lunetta, R.S. and **Williams, D.C.** 1992: Airborne multispectral scanner data for evaluating bottom sediment types and water depths of the St. Mary's River, Michigan. *Photogrammetric Engineering and Remote Sensing* 58, 951–56.

Lyzenga, D.R. 1978: Passive remote-sensing techniques for mapping water depth and bottom features. *Applied Optics* 17, 379–83.

— 1985: Shallow water bathymetry using combined lidar and passive multispectral scanner data. *International Journal of Remote Sensing* 6, 115–25.

Marcus, A.W., Legleiter, C.J., Aspinall, R.J., Boardman, J.W. and **Crabtree, R.L.** 2003: High spatial resolution hyperspectral mapping of in-stream habitats, depths, and woody debris in mountain streams. *Geomorphology* 55, 363–80.

McKean, J., Wright, W. and **Isaak, D.** 2006: Mapping channel morphology and stream habitat with a full waveform water-penetrating green lidar. In European Geosciences Union (EGU) General Assembly, 2–7 April, Vienna.

Melcher, N.B., Costa, J., Haeni, F., Cheng, R., Thurman, E., Buursink, M., Spicer, K., Hayes, E., Plant, W., Keller, W. and **Hayes, K.** 2002: River discharge measurements by using helicopter-mounted radar. *Geophysical Research Letters* 29(22), 2084, DOI: 10.1029/2002GL015525.

Mertes, L.A.K. 2002: Remote sensing of riverine landscapes. *Freshwater Biology* 47, 799–816.

Millar, D., Woolpert, J.G. and **Hilldale, R.** 2005: Using airborne lidar bathymetry to map shallow river environments. In Coastal GeoTools '05, 56–57.

Moorman, B.J. and **Michel, F.A.** 1997: Bathymetric mapping and sub-bottom profiling through lake ice with ground-penetrating radar. *Journal of Paleolimnology* 18, 61–73.

Morel, Y.G. 1998: Passive multispectral bathymetry mapping of Negril Shores, Jamaica. In Fifth International Conference on Remote Sensing for Marine and Coastal Environments, San Diego, 5–7 October.

Muirhead, K. and **Cracknell, A.** 1986: Airborne lidar bathymetry. *International Journal of Remote Sensing* 7, 597–614.

Muller, E., Decamps, H. and **Dobson, M.** 1993: Contribution of space remote sensing to river studies. *Freshwater Biology* 29, 301–12.

Okamoto, A. 1982: Wave influences in two-media photogrammetry. *Photogrammetric Engineering and Remote Sensing* 48, 1487–99.

Parson, L. Lillycrop, W. Klein, C. Ives, R. and **Orlando, S.** 1997: Use of lidar technology for collecting shallow water bathymetry of Florida Bay. *Journal of Coastal Research* 13, 1173–80.

Pe'eri, S. and **Philpot, W.** 2007: Increasing the existence of very shallow-water LIDAR measurements using the red-channel waveforms. *IEEE Transactions on Geosciences and Remote Sensing* 45, 1217–23.

Polcyn, F., Brown, W. and **Sattinger, I.** 1970: The measurement of water depth by remote sensing techniques (8973-26-F). Technical Report, Willow Run Laboratories, Ann Arbor, MI: University of Michigan.

Roberts, A. and **Anderson, J.** 1999: Shallow water bathymetry using integrated airborne multi-spectral remote sensing. *International Journal of Remote Sensing* 20, 497–510.

Schmugge, T. J., Kustas, W. P., Ritchie, J. C., Jackson, T. J. and **Rango, A.** 2002: Remote sensing in hydrology. *Advances in Water Resources* 25, 1367–85.

Spicer, K.R., Costa, J.E. and **Placzek, G.** 1997: Measuring flood discharge in unstable channels using ground-penetrating radar. *Geology* 25, 423–26.

Storlazzi, C., Logan, J. and **Field, M.** 2003: Quantitative morphology of a fringing reef tract from high-resolution laser bathymetry: Southern Molokai, Hawaii. *Bulletin of the Geological Society of America* 115, 1344–55.

Westaway, R., Lane, S. and **Hicks, D.** 2000: The development of an automated correction procedure for digital photogrammetry for the study of wide, shallow, gravel-bed rivers. *Earth Surface Processes and Landforms* 25, 209–26.

— 2001: Remote sensing of clear-water, gravel-bed rivers using digital photogrammetry. *Photogrammetric Engineering and Remote Sensing* 67, 1271–81.

— 2003: Remote survey of large-scale braided, gravel-bed rivers using digital photogrammetry and image analysis. *International Journal of Remote Sensing* 24, 795–815.

Winterbottom, S.J. and **Gilvear, D.J.** 1997: Quantification of channel bed morphology in gravel-bed rivers using airborne multispectral imagery and aerial photography. *Regulated Rivers: Research and Management* 13, 489–99.

Wozencraft, J. and **Millar, D.** 2005: Airborne lidar and integrated technologies for coastal mapping and nautical charting. *Marine Technology Society Journal* 39(3), 27–35.